

## Electron Transfer and Associative Detachment in Low-Temperature Collisions of $D^-$ with H

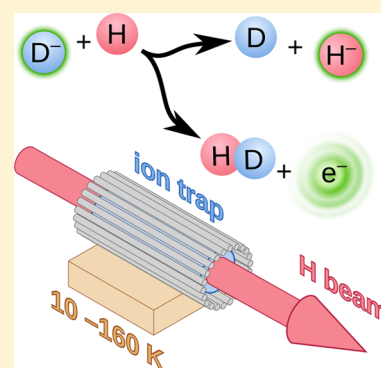
Štěpán Roučka,<sup>\*,†</sup> Dmytro Mulin,<sup>†</sup> Pavol Jusko,<sup>†</sup> Martin Čížek,<sup>‡</sup> Jiří Eliášek,<sup>‡</sup> Radek Plašil,<sup>†</sup> Dieter Gerlich,<sup>†,§</sup> and Juraj Glosík<sup>†</sup>

<sup>†</sup>Department of Surface and Plasma Science, Faculty of Mathematics and Physics, Charles University in Prague, Prague 180 00, Czech Republic

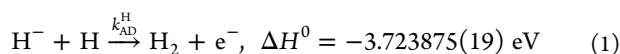
<sup>‡</sup>Institute of Theoretical Physics, Faculty of Mathematics and Physics, Charles University in Prague, Prague 180 00, Czech Republic

<sup>§</sup>Department of Physics, Technische Universität, 09107 Chemnitz, Germany

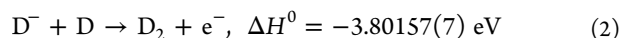
**ABSTRACT:** The interaction of  $D^-$  with H was studied experimentally and theoretically at low temperatures. The rate coefficients of associative detachment and electron transfer reactions were measured in the temperature range 10–160 K using a combination of a cryogenic 22-pole trap with a cold effusive beam of atomic hydrogen. Results from quantum-mechanical calculations are in good agreement with the experimental data. The rate coefficient obtained for electron transfer is increasing monotonically with temperature from  $1 \times 10^{-9} \text{ cm}^3 \text{ s}^{-1}$  at 10 K to  $5 \times 10^{-9} \text{ cm}^3 \text{ s}^{-1}$  at 160 K. The rate coefficient for associative detachment has a flat maximum of  $3 \times 10^{-9} \text{ cm}^3 \text{ s}^{-1}$  between 30 and 100 K.



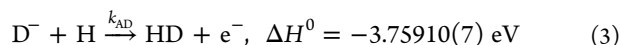
The associative detachment (AD) reaction of  $H^-$  with H



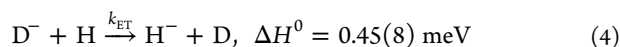
is the simplest anion-neutral reactive collision process. It has been studied by several theoretical approaches<sup>1–4</sup> and in various experiments.<sup>5–9</sup> The most recent measurements<sup>8,9</sup> confirm the rate coefficients calculated over a broad range of collision energies.<sup>4</sup> These studies were motivated by the role of reaction 1 as the main process for forming  $H_2$  in the late stages of the early universe.<sup>10</sup> A theoretical and experimental study of the deuterated variant of this reaction



found that the cross sections of both isotopic variants are identical within the error margins.<sup>11</sup> The present work is concerned with the asymmetric variant



which has not been studied experimentally until now. In addition to AD, this system can also react via the nearly resonant electron transfer (ET, or, more generally, charge transfer)



$k_{AD}^H$ ,  $k_{AD}$ , and  $k_{ET}$  are the rate coefficients for reactions 1, 3, and 4, respectively. Note that reaction 4 is weakly endothermic, which plays a role at very low temperatures. The enthalpies of

reactions at 0 K,  $\Delta H^0$ , were calculated from the dissociation energies of  $H_2$ , HD, and  $D_2$ <sup>12–14</sup> and from the electron affinities of H and D.<sup>15</sup>

Reaction 3 produces HD molecules, which play a significant role in the early universe. Despite its lower abundance, HD contributes to radiative cooling comparably to  $H_2$  due to the dipole moment and closer spacing of HD rotational levels.<sup>16,17</sup>

The symmetric ET process  $H^- + H \rightarrow H + H^-$  has been studied theoretically<sup>18,19</sup> and experimentally<sup>20,21</sup> using fast ion beams and stationary target at collision energies ranging from several electronvolts up to kiloelectronvolts. At low energies, the only way to distinguish between ET and elastic scattering is isotopic tagging. The asymmetric ET reactions  $D^- + H \rightarrow D + H^-$  and  $H^- + D \rightarrow H + D^-$  have been studied by means of crossed-beam method<sup>21,22</sup> at energies  $>4 \text{ eV}$ . The cross section for this process has not been previously calculated for the energies below a few electronvolts.

The measurements were carried out using the AB-22PT instrument (Atomic Beam with a 22-pole Trap),<sup>23</sup> which was also used to study the  $H^- + H$  reaction.<sup>9</sup> This device allows us to study the interaction of trapped ions with hydrogen atoms at low temperatures by combining the linear 22-pole radio-frequency ion trap<sup>24</sup> with an effusive source of atomic hydrogen.<sup>23</sup> The  $D^-$  ions were produced in a storage ion source<sup>25</sup> by electron bombardment of  $D_2$  precursor gas. After

Received: September 28, 2015

Accepted: November 12, 2015

Published: November 12, 2015

mass selection, the ions were injected into the trap and confined by a 27 MHz RF field with amplitudes up to 40 V applied to the rods. A detection system, consisting of a quadrupole mass filter, followed by a microchannel plate detector, is used to analyze the contents of the trap after a certain trapping time. The kinetic energy of trapped ions was thermalized by collisions with H<sub>2</sub> buffer gas. The ion kinetic temperature is close to the trap temperature,  $T_{\text{trap}}$ , which can be varied between 10 and 300 K (see discussion and references in Mulin et al.<sup>26</sup>). The D<sup>-</sup> ions may undergo the exchange reaction D<sup>-</sup> + H<sub>2</sub> → H<sup>-</sup> + HD, which is, however, slow due to a high potential barrier.<sup>27</sup> We have observed that the D<sup>-</sup> loss due to interaction with H<sub>2</sub> has a rate coefficient smaller than 10<sup>-15</sup> cm<sup>3</sup> s<sup>-1</sup> under the conditions of our experiment, making this process negligible.

The H atoms are produced via an inductively coupled RF discharge in pure hydrogen and cooled by flowing through a cold channel (accommodator) at temperatures  $T_{\text{acc}}$  in the range of 8 to 300 K.<sup>23</sup> The produced effusive beam passes along the trap axis, where the H atoms react with the trapped ions. Time-of-flight measurements have shown that the H-atom beam is well-characterized by a Maxwellian distribution with the temperature  $T_{\text{acc}}$ .<sup>23,28</sup>

In the AB-22PT instrument, the temperature of the ions and that of the H atoms are set separately. Therefore, collisions are characterized in the center of mass system of the colliding particles, defining the translational temperature

$$T_i = \frac{T_{\text{trap}}M_{\text{H}} + T_{\text{acc}}M_i}{M_{\text{H}} + M_i} \quad (5)$$

where  $M_i$  and  $M_{\text{H}}$  are the ion and H atom masses, respectively. Here we assume that the ion motion is really thermalized to  $T_{\text{trap}}$ . Note that the translational temperatures for collisions of H with simultaneously stored H<sup>-</sup> and D<sup>-</sup> are different. Also the effective number density of H atoms (denoted  $N_{\text{H}}^i$ ) experienced by the ions depends on the ion mass. For a given number density of ions in the trap,  $n_i$ ,  $N_{\text{H}}^i$  is given by the overlap integral  $N_{\text{H}}^i = \int n_{\text{H}}(r) \frac{n_i(r)}{N_i} d^3r$ , where  $n_{\text{H}}$  is the number density of H atoms in the beam and  $N_i$  is the total number of trapped ions. Two methods were used to calibrate  $N_{\text{H}}^i$ , necessary for obtaining absolute reaction rate coefficients. The first method is based on chemical probing of the H number density using the previously studied reaction CO<sub>2</sub><sup>+</sup> + H → HCO<sup>+</sup> + O, which has a known reaction rate coefficient.<sup>23</sup> This calibrating method has systematic uncertainty of 40%, as discussed in previous works.<sup>9,28</sup> The other method is based on the known theoretical value<sup>4</sup> of the rate coefficient for reaction 1, which is in good agreement with recent measurements.<sup>8,9</sup> On the basis of the spread of the independently measured and calculated values, we estimate that the systematic error of this calibration will be <30%. Both calibration methods will be compared.

For describing the changes in the number of trapped ions,  $N_{\text{H}}^{\text{H}^-}$  and  $N_{\text{D}}^{\text{D}^-}$ , and for correlating them with the actually detected numbers,  $N_{\text{H}}^-$  and  $N_{\text{D}}^-$ , we need to account for their slightly different detection efficiencies,  $\alpha_{\text{H}^-}$  and  $\alpha_{\text{D}^-}$ , defined by  $N_{\text{D}}^- = \alpha_{\text{D}^-} N_{\text{D}}^{\text{D}^-}$  and  $N_{\text{H}}^- = \alpha_{\text{H}^-} N_{\text{H}}^{\text{H}^-}$ . Using this and the previously defined ion-dependent H atom densities, one obtains the coupled kinetic equations

$$\frac{dN_{\text{D}}^-}{dt} = -k_{\Sigma} N_{\text{D}}^- N_{\text{H}}^{\text{D}^-} \quad (6)$$

$$\frac{dN_{\text{H}}^-}{dt} = -k_{\text{AD}}^{\text{H}} N_{\text{H}}^- N_{\text{H}}^{\text{H}^-} + k_{\text{ET}} \frac{\alpha_{\text{H}^-}}{\alpha_{\text{D}^-}} N_{\text{D}}^- N_{\text{H}}^{\text{D}^-} \quad (7)$$

where  $k_{\Sigma} = k_{\text{AD}} + k_{\text{ET}}$  denotes the overall rate coefficient for the D<sup>-</sup> + H reaction. The factor  $\alpha_{\text{H}^-}/\alpha_{\text{D}^-}$  corrects for the fact that the kinetics has to be written down for the actually stored number of ions.

As a typical result, Figure 1 shows the changes of the number of detected ions as a function of time at different combinations

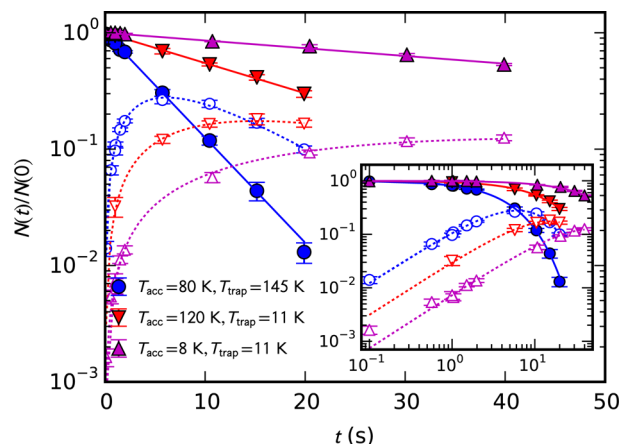


**Figure 1.** Time evolution of normalized numbers of detected D<sup>-</sup> ions (filled symbols) and H<sup>-</sup> ions (open symbols) at different combinations of  $T_{\text{acc}}$  and  $T_{\text{trap}}$ . The solid and dashed lines show solutions of eq 6 and 7 fitted to the data. The inset shows the same data with logarithmic time axis.

of  $T_{\text{acc}}$  and  $T_{\text{trap}}$ . The normalized number of initially injected D<sup>-</sup> ions decreases monotonously, while the number of H<sup>-</sup> products increases in the first seconds until the loss via associative detachment takes over. The data were analyzed by least-squares fitting the unknown rates in eqs 6 and 7. To eliminate the difference between  $N_{\text{H}}^{\text{H}^-}$  and  $N_{\text{H}}^{\text{D}^-}$ , the time evolutions were obtained at RF amplitudes scaled with the square root of ion mass of D<sup>-</sup> and H<sup>-</sup>, which leads to equivalent effective potentials<sup>25</sup> (typical amplitudes were 29 V for fitting  $k_{\Sigma} N_{\text{H}}^{\text{D}^-}$  and  $k_{\text{ET}} N_{\text{H}}^{\text{D}^-} \alpha_{\text{H}^-}/\alpha_{\text{D}^-}$  and 21 V for fitting  $k_{\text{AD}}^{\text{H}} N_{\text{H}}^{\text{H}^-}$ ). Hence we can assume  $N_{\text{H}} \equiv N_{\text{H}}^{\text{H}^-} = N_{\text{H}}^{\text{D}^-}$  at any given combination of temperatures  $T_{\text{trap}}$  and  $T_{\text{acc}}$ . The a priori unknown temperature dependence of  $N_{\text{H}}$  was eliminated by calculating rate ratios  $k_{\Sigma}/k_{\text{AD}}^{\text{H}}$  and  $\alpha_{\text{H}^-}/\alpha_{\text{D}^-} \cdot k_{\text{ET}}/k_{\Sigma}$ .

The ratios  $k_{\Sigma}/k_{\text{AD}}^{\text{H}}$  as a function of D<sup>-</sup> + H translational temperature are plotted in Figure 2a (triangles). It was observed that at  $T_{\text{trap}} < 50$  K, the ratios  $k_{\Sigma}/k_{\text{AD}}^{\text{H}}$  depend on  $T_{\text{trap}}$  even if constant translational temperature is maintained. This appears to be a violation of our assumption that  $N_{\text{H}}^{\text{H}^-} = N_{\text{H}}^{\text{D}^-}$  when the same effective potential is used. It is due to sensitivity of the ion distribution to small surface potential perturbations modifying the effective potential by some millielectronvolts. By comparing the ratios measured at identical translational temperatures with  $T_{\text{trap}} = 11$  K and with  $T_{\text{trap}} > 80$  K, we found that the ratio of effective number densities is  $N_{\text{H}}^{\text{H}^-}/N_{\text{H}}^{\text{D}^-} = 1.63 \pm 0.16$  at  $T_{\text{trap}} = 11$  K. The ratios  $k_{\Sigma}/k_{\text{AD}}^{\text{H}}$  obtained at  $T_{\text{trap}} = 11$  K were multiplied by this factor (plotted as open circles in Figure 2a). Intermediate trap

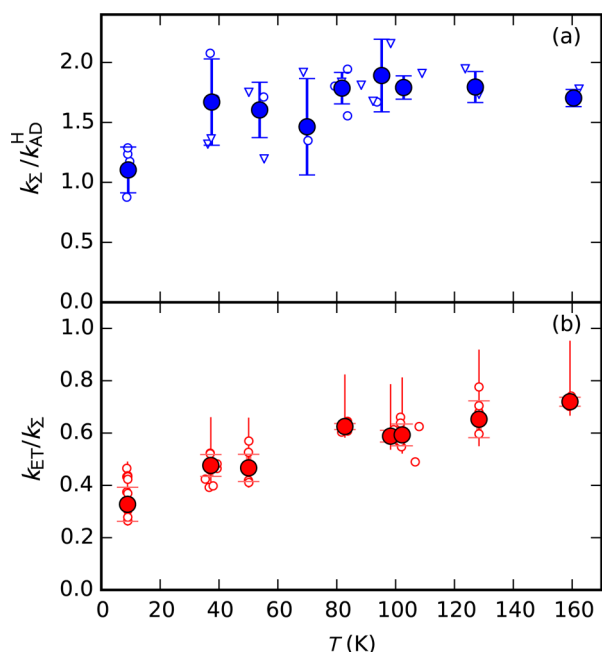


**Figure 2.** (a) Ratio between  $k_{\Sigma}$  (reaction  $D^- + H$ ) and  $k_{AD}^H$  (reaction  $H^- + H$ ) as a function of temperature. The data obtained at  $T_{\text{trap}} > 80$  K are indicated by open triangles. The open circles indicate the data measured at  $T_{\text{trap}} = 11$  K corrected for difference between  $N_{\text{H}}^{\text{H}^-}$  and  $N_{\text{H}}^{\text{D}^-}$ . The filled symbols show the averaged data after binning. (b) Ratio of the electron-transfer rate coefficient  $k_{\text{ET}}$  and the overall reaction rate coefficient  $k_{\Sigma}$  as a function of temperature. The filled symbols show the binned data. The statistical and systematic + statistical uncertainties are indicated by the inner and outer error bars, respectively.

temperatures  $11 \text{ K} < T_{\text{trap}} < 80 \text{ K}$  were not used in the present experiment.

The branching ratios  $k_{\text{ET}}/k_{\Sigma}$  for reaction 4 (plotted in Figure 2b) have been obtained by accounting for the discrimination factor  $\alpha_{\text{H}^-}/\alpha_{\text{D}^-}$ . We used the reaction of  $D^+ + \text{H}_2 \rightarrow \text{H}^+ + \text{HD}$  to measure the mass discrimination by converting  $D^+$  to  $H^+$ . The obtained values of the discrimination factor  $\alpha_{\text{H}^-}/\alpha_{\text{D}^-}$  for various configurations of the detection system differ from unity by up to +5 or -23% in both directions. We assume that the discrimination for negative ions will also be of this value because the MCP detection efficiency is almost the same for both isotopes<sup>29</sup> and the ion trapping and extraction potentials were equivalent. This leads to the asymmetric systematic uncertainty of the measured branching ratio in Figure 2.

Absolute values for the reaction rate coefficients  $k_{\Sigma}$  were obtained by calibrating the  $N_{\text{H}}$  as previously described. The results based on  $\text{CO}_2^+$  chemical probing (yielding typical effective densities  $N_{\text{H}} = 2.5 \times 10^7 \text{ cm}^{-3}$ ) and on multiplying the ratios  $k_{\Sigma}/k_{AD}^H$  with theoretical values of  $k_{AD}^H$  are indicated in Figure 3 by stars and circles, respectively. Within the errors, both methods lead to the same result. These results are in good agreement with our theoretical values for  $D^- + H$  below 120 K as well. Figure 3 also presents previous measured and calculated associative detachment rate coefficients of  $H^- + H$  and  $D^- + D$ . Note that the  $D^- + D$  and  $H^- + H$  rate coefficients are just for associative detachment, while  $k_{\Sigma}$  for  $D^- + H$  also includes the electron transfer.

For separating the ET and AD rate coefficients (plotted in Figure 4), all data were binned in temperature to facilitate the

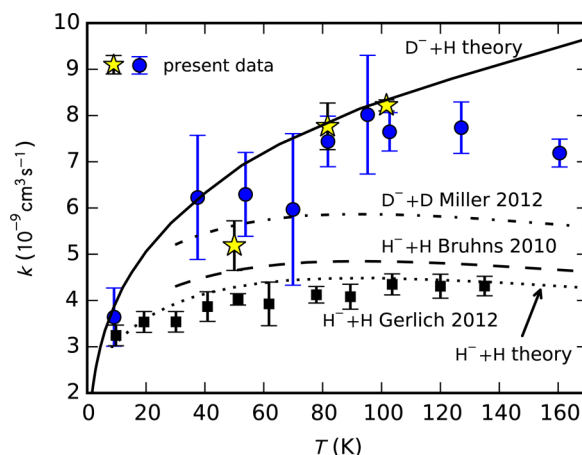


**Figure 3.** Measured and calculated reaction rate coefficients for three different isotopic variants of the  $H^- + H$  system plotted as a function of the respective translational temperatures. The present experimental data for  $k_{\Sigma}$  (circles and stars, see text for details) are compared with the new theoretical values (solid line). The measured (squares,<sup>9</sup> dashed line<sup>30</sup>) and calculated (dotted line<sup>31</sup>) rate coefficients  $k_{AD}^H$  of  $H^- + H$  and the measured rate coefficient  $k_{AD}$  of  $D^- + D$  (dashed-dotted line<sup>11</sup>) are shown for comparison.

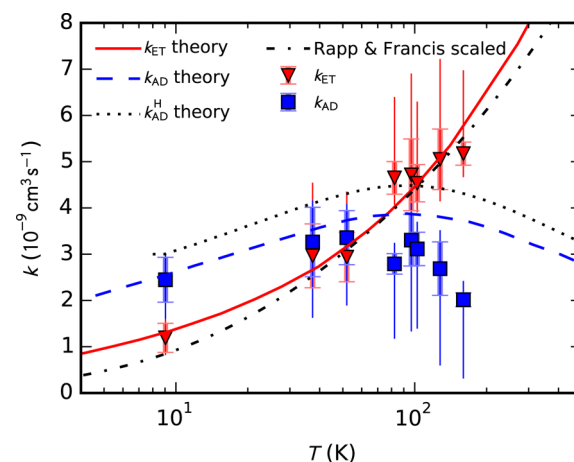


**Figure 4.** Rate coefficients for AD and ET in  $D^- + H$  collisions as a function of translational temperature. The experimental data are shown as squares ( $k_{AD}$ ) and triangles ( $k_{\text{ET}}$ ), and the calculated results are shown as dashed ( $k_{AD}$ ) and solid ( $k_{\text{ET}}$ ) lines. The statistical uncertainties and the systematic uncertainties due to discrimination are indicated by the inner and outer error bars. For comparison, we show theoretical  $k_{AD}^H$  (dotted line<sup>4</sup>) and  $k_{\text{ET}}$  according to the Rapp and Francis theory<sup>32</sup> scaled by 1/3.6 (dashed-dotted line).

multiplication of data sets.  $k_{\text{ET}}$  was calculated as a product of the total reaction rate coefficient (Figure 3) and the branching ratio (Figure 2b).  $k_{AD}$  was obtained by subtracting the  $k_{\text{ET}}$  from the total rate coefficient  $k_{\Sigma}$ . Inspection of Figure 4 reveals that electron transfer is the dominant process at higher temperatures. Consequently,  $k_{AD}$  has large error estimates, especially due to the uncertainty of mass discrimination. Theoretical curves calculated as explained in the Computational Methods are also shown in Figure 4.

To get some insight into the electron-transfer process, we also used the simple Rapp and Francis theory.<sup>32</sup> The calculated rate coefficient is more than 3 times higher than the present results; however, after scaling with factor 1/3.6 it reproduces the energy dependence of our data rather well. The failure to

obtain a good absolute value for the rate is not surprising because it uses oversimplified electron wave function and ignores the detachment channel and the polarization. The previously calculated  $k_{AD}^H$ <sup>4</sup> is also shown in Figure 4. The rate coefficients of AD of the different isotopic variants differ only by the square root of reduced mass ratio factor; that is, the cross sections of both processes are almost identical. This has been previously observed in comparison of the  $D^- + D$  and  $H^- + H$  AD rate coefficients.<sup>11</sup>

To conclude, we presented the first study of  $D^- + H$  reaction at temperatures below 300 K. The measured total reaction rate coefficient (Figure 3) is in good agreement with the theory below 120 K. The decline of measured  $k_{\Sigma}$  may be caused partly by influence of evaporative loss of  $H^-$  on the calibration at higher temperatures. Inspection of Figure 4 reveals that associative detachment dominates at low temperatures, reaching a maximum at  $\sim 50$  K. With increasing temperatures, the electron-transfer rate coefficient increases monotonously and becomes dominant, a typical behavior of electron-transfer processes occurring at large impact parameters.<sup>32</sup> At relevant temperatures, the theoretical cross sections for AD of  $H^- + H$  and  $D^- + H$  are nearly identical and the differences in reaction rate coefficients are simply due to the different thermal velocities of  $D^-$  and  $H^-$ . Above 70 K our experimental data for  $k_{AD}$  start to deviate from theory. The discrepancy may be partly due to uncertainty of the discrimination, which is indicated by the error bars. Another reason may be the mentioned evaporative loss of  $H^-$  ions. A comparison of the  $D^- + H$  system with  $H^- + D$  may shed more light onto these issues.

The comparison of the two channels may also be important for the development of the theory. Note that in the theoretical treatment (described in the Computational Methods), the small energy difference between  $D^- + H$  and  $H^- + D$  channels is not taken into account. We are planning to clarify the influence of this correction on the competition between AD and ET reaction channels at low energies. Investigating the differences between the endothermic  $D^- + H$  and the exothermic  $H^- + D$  will, therefore, be of interest both for the theory and for the experiment.

## COMPUTATIONAL METHODS

The theoretical description of the associative detachment (eq 3) and the electron-transfer (eq 4) processes is closely related because they both involve the evolution of the same initial state. We have treated the  $^2\Sigma_u$  state contribution to associative detachment reaction in  $H^- + H$  previously beyond the local complex potential approximation,<sup>4</sup> and more recently we have also included the repulsive  $^2\Sigma_g$  state for  $H^- + H$  and  $D^- + D$  collisions.<sup>11,33</sup> The contribution from the  $^2\Sigma_g$  state is only a small correction for the associative detachment process. For the electron transfer both  $^2\Sigma_u$  and  $^2\Sigma_g$  states are needed because both the initial and final channels with the localized electron are a 1:1 mixture of both gerade and ungerade states. Because the parity of the state is conserved during the collision we can calculate the radial wave function  $\psi_u(R)$  and  $\psi_g(R)$  for ungerade and gerade electronic states separately. We will use atomic units in the formulas of this section. The wave functions solve the effective radial Schrödinger equation

$$\left\{ \frac{d^2}{dR^2} + k^2 - U_s - \frac{l(l+1)}{R^2} - \hat{F}_s \right\} \psi_s = 0 \quad (8)$$

where  $s = u, g$  stands for the ungerade and gerade contribution, respectively,  $E = k^2/2m$  is the kinetic energy of the collision,  $V_s(R) = U_s(R)/2m$  is the potential energy,  $m$  is the reduced mass,  $l$  is the orbital angular momentum quantum number, and

$$\hat{F}_s(E) = 2m \int V_{de}^{(s)} \left[ E - \epsilon - \frac{\Delta}{2m} - V_0(R) - i\eta \right]^{-1} V_{de}^{(s)*} d\epsilon \quad (9)$$

is the nonlocal potential due to interaction of the discrete ionic state  $HD^-$  with the electron continuum  $HD + e^-$ .  $\eta$  denotes a positive infinitesimal. This potential depends on the potential energy curve  $V_0(R)$  for the neutral molecule (only the ground state is considered because excited states contribute negligibly) and on the element  $V_{de}^{(s)}$  coupling the anion state and the electron continuum. The integration is carried out over all possible energies  $\epsilon$  and the other quantum numbers uniquely determining the state of the released electron. The nonlocal potential has often been replaced with the local complex potential approximation  $F_s(R) = D_s(R) - i\Gamma_s(R)/2$ , where  $D_s(R)$  is the correction of the potential energy  $U_s(R)$  and  $\Gamma_s(R)$  is the local autodetachment width responsible for the electron detachment.<sup>1,19</sup> In our treatment the full nonlocal, energy-dependent form of  $F_s$  given by the integral expression above is taken into account. The radial Schrödinger equation is solved in its integral form (Lippmann–Schwinger equation) to include the proper scattering boundary conditions.<sup>4</sup> The functions  $U_g$ ,  $U_w$ ,  $F_g$ , and  $F_u$  determining the model were derived as in Miller et al.<sup>33</sup> using the procedure of Belyaev et al.<sup>34</sup> The cross sections for the electron-transfer process were calculated from the difference between the elastic contributions to the  $T$ -matrix for gerade and ungerade symmetry, which is equivalent to the formula

$$\sigma_{ET} = \frac{\pi}{k^2} \sum_l (2l+1) \left| \sin(\delta_g - \delta_u) e^{i(\delta_g + \delta_u)} \right|^2 \quad (10)$$

where the phase shifts  $\delta_s$  are extracted from the asymptotic form of the wave function

$$\psi_s(S) \xrightarrow{R \rightarrow \infty} A_s \sin\left(kR - \frac{\pi}{2}l + \delta_s\right) \quad (11)$$

for large  $R$ . Note that the phase shifts  $\delta_s$  are complex numbers due to contribution of the electron detachment process. The detailed results of the calculation including differential cross sections will be discussed elsewhere. Here we have calculated the integral electron transfer cross section for the energy range 0.1 meV to 1 eV. It is nearly constant ( $250 \text{ \AA}^2$ ) for energies below 0.1 eV, with small modulation (up to 20%) due to resonances related to series of long-lived  $HD^-$  anionic states.<sup>31</sup> For larger energies the cross section starts to decrease in accordance with previous calculations.<sup>18,19</sup> It should be mentioned that for lower temperatures this model is not accurate as we neglect nonadiabatic effects that differentiate energy of  $D^- + H$  and  $H^- + D$  (0.45 meV). So the results at the low temperature ( $< 10$  K) should be taken only as an approximation.

To compare the prediction of the theory with the data measured in the present experiment, we finally averaged the integral cross section multiplied by velocity over the Maxwell–Boltzmann distribution. The associative detachment cross section can be calculated using the same method as described by Miller et al.<sup>11</sup> or again from the phase shifts  $\delta_s$  using the formula

$$\sigma_{AD} = \frac{\pi}{k^2} \sum_l (2l+1) [2 - \exp(-4\text{Im} \delta_u) - \exp(-4\text{Im} \delta_g)] \quad (12)$$

for the total cross section of absorption on the nonhermitian potential  $F_s$  (summed over gerade and ungerade contribution).

## AUTHOR INFORMATION

### Corresponding Author

\*Phone: +420 22191 2344. E-mail: [Stepan.Roucka@mff.cuni.cz](mailto:Stepan.Roucka@mff.cuni.cz).

### Notes

The authors declare no competing financial interest.

## ACKNOWLEDGMENTS

The 22-pole ion trap instrument has been developed in Chemnitz, and since 2010 it has been operated at the Faculty of Mathematics and Physics of the Charles University in Prague. We thank the Technische Universität Chemnitz and the Deutsche Forschungsgemeinschaft for making this transfer possible. This work was partly supported by GACR (P209/12/0233, 14-14715P, 208/10/1281), GAUK 572214, and UNCE-204020.

## REFERENCES

- Browne, J. C.; Dalgarno, A. Detachment in Collisions of H and H<sup>-</sup>. *J. Phys. B: At. Mol. Phys.* **1969**, *2*, 885.
- Bieniek, R. J.; Dalgarno, A. Associative Detachment in Collisions of H and H<sup>-</sup>. *Astrophys. J.* **1979**, *228*, 635–639.
- Sakimoto, K. Ion–molecule Reactions at Extremely Low Energies: H<sup>-</sup> + H → H<sub>2</sub> + e. *Chem. Phys. Lett.* **1989**, *164*, 294–298.
- Čížek, M.; Horáček, J.; Domcke, W. Nuclear Dynamics of the H<sub>2</sub><sup>-</sup> Collision Complex Beyond the Local Approximation: Associative Detachment and Dissociative Attachment to Rotationally and Vibrationally Excited Molecules. *J. Phys. B: At. Mol. Opt. Phys.* **1998**, *31*, 2571–2583.
- Schmeltekopf, A. L.; Fehsenfeld, F. C.; Ferguson, E. E. Laboratory Measurement of the Rate Constant for H<sup>-</sup> + H → H<sub>2</sub> + e. *Astrophys. J.* **1967**, *148*, L155–L156.
- Fehsenfeld, F. C.; Howard, C. J.; Ferguson, E. E. Thermal Energy Reactions of Negative Ions with H Atoms in the Gas Phase. *J. Chem. Phys.* **1973**, *58*, 5841–5842.
- Martinez, O.; Yang, Z.; Betts, N. B.; Snow, T. P.; Bierbaum, V. M. Experimental Determination of the Rate Constant for the Associative Detachment Reaction H<sup>-</sup> + H → H<sub>2</sub> + e<sup>-</sup> at 300 K. *Astrophys. J.* **2009**, *705*, L172–L175.
- Kreckel, H.; Bruhns, H.; Čížek, M.; Glover, S. C. O.; Miller, K. A.; Urbain, X.; Savin, D. W. Experimental Results for H<sub>2</sub> Formation from H<sup>-</sup> and H and Implications for First Star Formation. *Science* **2010**, *329*, 69–71.
- Gerlich, D.; Jusko, P.; Roučka, Š.; Zymak, I.; Plašil, R.; Glosík, J. Ion Trap Studies of H<sup>-</sup> + H → H<sub>2</sub> + e<sup>-</sup> Between 10 and 135 K. *Astrophys. J.* **2012**, *749*, 22.
- Glover, S. C.; Savin, D. W.; Jappsen, A. K. Cosmological Implications of the Uncertainty in H<sup>-</sup> Destruction Rate Coefficients. *Astrophys. J.* **2006**, *640*, 553–568.
- Miller, K.; Bruhns, H.; Čížek, M.; Eliášek, J.; Cabrera-Trujillo, R.; Kreckel, H.; O'Connor, A.; Urbain, X.; Savin, D. Isotope Effect for Associative Detachment: H(D)<sup>-</sup> + H(D) → H<sub>2</sub>(D<sub>2</sub>) + e<sup>-</sup>. *Phys. Rev. A: At., Mol., Opt. Phys.* **2012**, *86*, 032714.
- Liu, J.; Salumbides, E. J.; Hollenstein, U.; Koelemeij, J. C. J.; Eikema, K. S. E.; Ubachs, W.; Merkt, F. Determination of the Ionization and Dissociation Energies of the Hydrogen Molecule. *J. Chem. Phys.* **2009**, *130*, 174306.
- Sprecher, D.; Liu, J.; Jungen, C.; Ubachs, W.; Merkt, F. Communication: The Ionization and Dissociation Energies of HD. *J. Chem. Phys.* **2010**, *133*, 111102.
- Liu, J.; Sprecher, D.; Jungen, C.; Ubachs, W.; Merkt, F. Determination of the Ionization and Dissociation Energies of the Deuterium Molecule (D<sub>2</sub>). *J. Chem. Phys.* **2010**, *132*, 154301.
- Lykke, K. R.; Murray, K. K.; Lineberger, W. C. Threshold Photodetachment of H<sup>-</sup>. *Phys. Rev. A: At., Mol., Opt. Phys.* **1991**, *43*, 6104–6107.
- Flower, D. R.; Pineau des Forêts, G. The Thermal Balance of the First Structures in the Primordial Gas. *Mon. Not. R. Astron. Soc.* **2001**, *323*, 672–676.
- Nakamura, F.; Umemura, M. The Stellar Initial Mass Function in Primordial Galaxies. *Astrophys. J.* **2002**, *569*, 549.
- Dalgarno, A.; McDowell, M. R. C. Charge Transfer and the Mobility of H<sup>-</sup> Ions in Atomic Hydrogen. *Proc. Phys. Soc., London, Sect. A* **1956**, *69*, 615.
- Bardsley, J. N. Electron Detachment and Charge Transfer in H–H<sup>-</sup> Collisions. *Proc. Phys. Soc., London* **1967**, *91*, 300.
- Hummer, D. G.; Stebbings, R. F.; Fite, W. L.; Branscomb, L. M. Charge Transfer and Electron Production in H<sup>-</sup> + H Collisions. *Phys. Rev.* **1960**, *119*, 668–670.
- Huels, M. A.; Champion, R. L.; Doverspike, L. D.; Wang, Y. Charge Transfer and Electron Detachment for Collisions of H<sup>-</sup> and D<sup>-</sup> with H. *Phys. Rev. A: At., Mol., Opt. Phys.* **1990**, *41*, 4809–4815.
- Esaulov, V. A. Electron Detachment and Charge Exchange in H<sup>-</sup> Scattering by Atomic Deuterium. *J. Phys. B: At. Mol. Phys.* **1980**, *13*, 4039.
- Borodi, G.; Luca, A.; Gerlich, D. Reactions of CO<sub>2</sub><sup>+</sup> with H, H<sub>2</sub> and Deuterated Analogues. *Int. J. Mass Spectrom.* **2009**, *280*, 218–225.
- Gerlich, D.; Horning, S. Experimental Investigation of Radiative Association Processes as Related to Interstellar Chemistry. *Chem. Rev.* **1992**, *92*, 1509–1539.
- Gerlich, D. Inhomogeneous RF Fields: a Versatile Tool for the Study of Processes with Slow Ions. *Adv. Chem. Phys.* **1992**, *82*, 1.
- Mulin, D.; Roučka, Š.; Jusko, P.; Zymak, I.; Plašil, R.; Gerlich, D.; Wester, R.; Glosík, J. H/D Exchange in Reactions of OH<sup>-</sup> with D<sub>2</sub> and of OD<sup>-</sup> with H<sub>2</sub> at Low Temperatures. *Phys. Chem. Chem. Phys.* **2015**, *17*, 8732–8739.
- Haufler, E.; Schlemmer, S.; Gerlich, D. Absolute Integral and Differential Cross Sections for the Reactive Scattering of H<sup>-</sup> + D<sub>2</sub> and D<sup>-</sup> + H<sub>2</sub>. *J. Phys. Chem. A* **1997**, *101*, 6441–6447.
- Plašil, R.; Mehner, T.; Dohnal, P.; Kotrík, T.; Glosík, J.; Gerlich, D. Reactions of Cold Trapped CH<sup>+</sup> Ions with Slow H Atoms. *Astrophys. J.* **2011**, *737*, 60.
- Peko, B. L.; Stephen, T. M. Absolute Detection Efficiencies of Low Energy H, H<sup>-</sup>, H<sup>+</sup>, H<sub>2</sub><sup>+</sup> and H<sub>3</sub><sup>+</sup> Incident on a Multichannel Plate Detector. *Nucl. Instrum. Methods Phys. Res., Sect. B* **2000**, *171*, 597–604.
- Bruhns, H.; Kreckel, H.; Miller, K. A.; Urbain, X.; Savin, D. W. Absolute Energy-Resolved Measurements of the H<sup>-</sup> + H → H<sub>2</sub> + e<sup>-</sup> Associative Detachment Reaction Using a Merged-Beam Apparatus. *Phys. Rev. A: At., Mol., Opt. Phys.* **2010**, *82*, 042708.
- Čížek, M.; Horáček, J.; Domcke, W. Long-Lived Anionic States of H<sub>2</sub>, HD, D<sub>2</sub>, and T<sub>2</sub>. *Phys. Rev. A: At., Mol., Opt. Phys.* **2007**, *75*, 012507.
- Rapp, D.; Francis, W. E. Charge Exchange between Gaseous Ions and Atoms. *J. Chem. Phys.* **1962**, *37*, 2631–2645.
- Miller, K. A.; Bruhns, H.; Eliášek, J.; Čížek, M.; Kreckel, H.; Urbain, X.; Savin, D. W. Associative Detachment of H<sup>-</sup> + H → H<sub>2</sub> + e<sup>-</sup>. *Phys. Rev. A: At., Mol., Opt. Phys.* **2011**, *84*, 052709.
- Belyaev, A. K.; Tiukanov, A. S.; Domcke, W. Generalized Diatomics-In-Molecule Method Applied to the H<sub>3</sub><sup>-</sup> Anion. *Chem. Phys.* **2006**, *325*, 378–388.